

Supporting Information:
**Raising the benchmark potential of a simple
alcohol-ketone intermolecular balance**

Ch. Zimmermann, A. C. Dorst, M. A. Suhm*

E-mail: msuhm@gwdg.de

Contents

1	Theoretical results	S-1
1.1	Monomers	S-2
1.2	Dimers	S-6
2	Experimental Results	S-11
2.1	Methyl-ethyl-ketone (MEK) + MeOH	S-14
2.2	Ethyl-ethyl-ketone (EEK) + MeOH	S-19
3	Comparison Experiment vs. Theory	S-22
	References	S-26

1 Theoretical results

Tab. S1: ORCA 4.2.1^{S1} and Turbomole^{S2,S3} keywords used for the different electronic structure optimizations, transition state searches (superscript TS) and relaxed scans (superscript RS). D3-parameters for X3LYP were taken from literature.^{S4}

Level of approximation	Employed keywords
B3LYP-D3(BJ,ABC)/def2-TZVP (ORCA)	B3LYP D3BJ def2-TZVP abc grid5 NoFinalGrid UseSym VERYTIGHTSCF TIGHTOPT FREQ
B3LYP-D3(BJ,ABC)/def2-TZVP (ORCA) ^{TS}	B3LYP D3BJ def2-TZVP abc grid5 NoFinalGrid UseSym OptTS VERYTIGHTSCF TIGHTOPT FREQ
B3LYP-D3(BJ,ABC)/def2-QZVP (ORCA)	B3LYP D3BJ def2-QZVPP abc grid5 NoFinalGrid UseSym VERYTIGHTSCF TIGHTOPT FREQ
X3LYP/def2-TZVP (ORCA)	X3LYP def2-TZVP grid5 NoFinalGrid UseSym VERYTIGHTSCF TIGHTOPT FREQ
X3LYP-D3(BJ,ABC)/def2-TZVP (ORCA)	X3LYP D3BJ def2-TZVP abc grid5 NoFinalGrid UseSym VERYTIGHTSCF TIGHTOPT FREQ
DLPNO-CCSD(T) (ORCA)	DLPNO-CCSD(T) TightPNO aug-cc-pVQZ aug-cc-pVQZ/C TightSCF LED
BP86-D3(BJ,ABC)/def2-TZVP (ORCA)	BP86 D3BJ def2-TZVP abc grid5 NoFinalGrid UseSym VERYTIGHTSCF TIGHTOPT FREQ
B3LYP-D3(BJ,ABC)/def2-TZVP (TURBOMOLE) ^{RS,TS}	b3-lyp def2-mTZVP grid m5 disp3 bj abc ri
B3LYP-D3(BJ,ABC)/def2-QZVP (TURBOMOLE) ^{RS}	b3-lyp def2-QZVPP grid m5 disp3 bj abc ri

1.1 Monomers

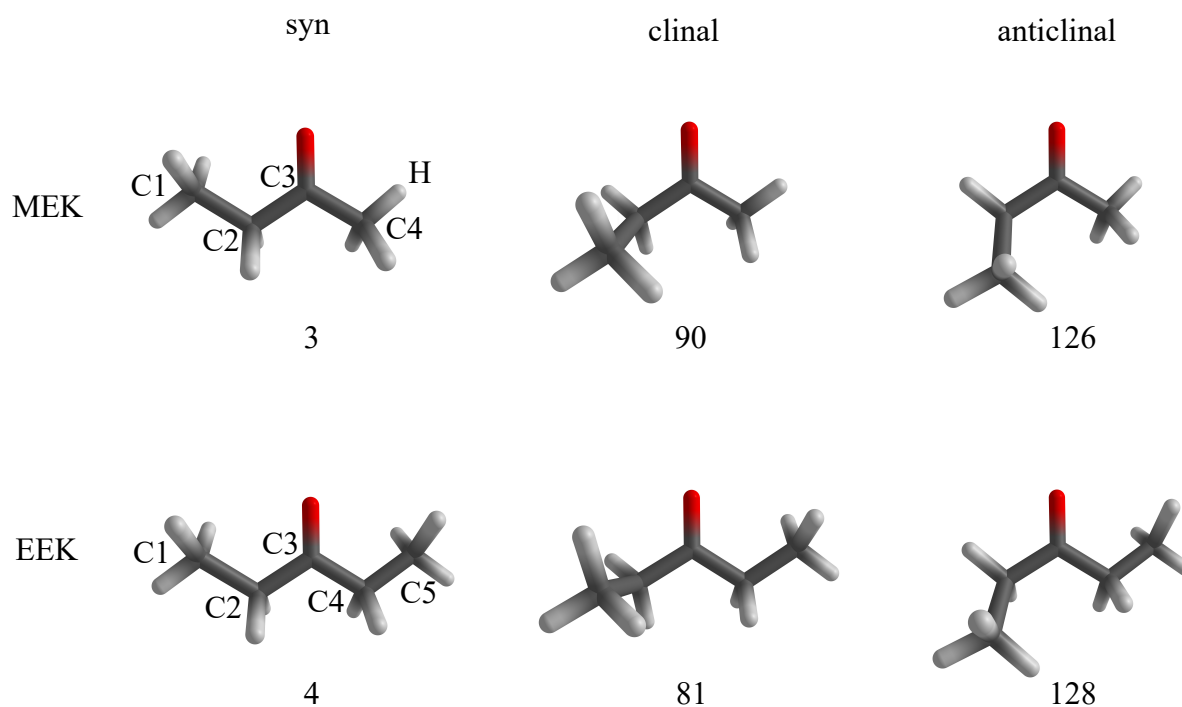


Fig. S1: Structures of the three most stable monomeric methyl-ethyl-ketone (MEK) and ethyl-ethyl-ketone (EEK) isomers at B3LYP-D3(BJ,ABC)/def2-TZVP level where syn, clinal and anticlinal are derived from the Newman Projection^{S5} for the ethyl group relative to the carbonyl bond. Also given is the O=C3C2C1 ethyl dihedral angle $\tau_{\text{mono}}^{\text{O}=\text{C}3\text{C}2\text{C}1}$ in $^{\circ}$ (see also table S2). The electronic energy increases with increasing $\tau_{\text{mono}}^{\text{O}=\text{C}3\text{C}2\text{C}1}$ (see table S2). The three structure motifs can be found in both systems, underlining the similarity of the two molecules. Two further EEK isomers with torsion in both ethyl groups lie above 10 kJ mol^{-1} . They are therefore not presented and excluded from the subsequent discussion.

Tab. S2: Energetic isomer sequence in methyl-ethyl-ketone (MEK) and ethyl-ethyl-ketone (EEK) structures (naming after Newman Projection (NP))^{S5} predicted by B3LYP-D3(BJ,ABC)/def2-TZVP or X3LYP-D3(BJ,ABC)/def2-TZVP in kJ mol⁻¹ relative to the most stable conformer syn. ΔE^0 includes the harmonically approximated zero-point energy and ΔE^{el} excludes it. Also, the dihedral angles $\tau_{\text{mono}}^{\text{O=C3C2C1}}$ and $\tau_{\text{mono}}^{\text{O=C3C4H/C5}}$ (always syn) are given in °. The similarity of the two systems and the two density functional variants is evident from the structural and energetic results.

Ketone	NP	Method	$\Delta E_{\text{NP-syn}}^{\text{el}}$	$\Delta E_{\text{NP-syn}}^0$	$\tau_{\text{mono}}^{\text{O=C3C2C1}}$	$\tau_{\text{mono}}^{\text{O=C3C4H/C5}}$
MEK	syn	B3LYP-D3(BJ)	0.00	0.00	3	6
	clinal		4.68	5.93	90	10
	antichinal		5.13	6.27	126	15
MEK	syn	X3LYP-D3(BJ)	0.00	0.00	3	6
	clinal		4.80	6.06	90	10
	antichinal		5.01	6.20	127	15
EEK	syn	B3LYP-D3(BJ)	0.00	0.00	4	4
	clinal		3.83	4.85	81	6
	antichinal		5.35	6.34	128	9
EEK	syn	X3LYP-D3(BJ)	0.00	0.00	4	4
	clinal		3.69	4.99	82	6
	antichinal		5.22	6.27	129	10

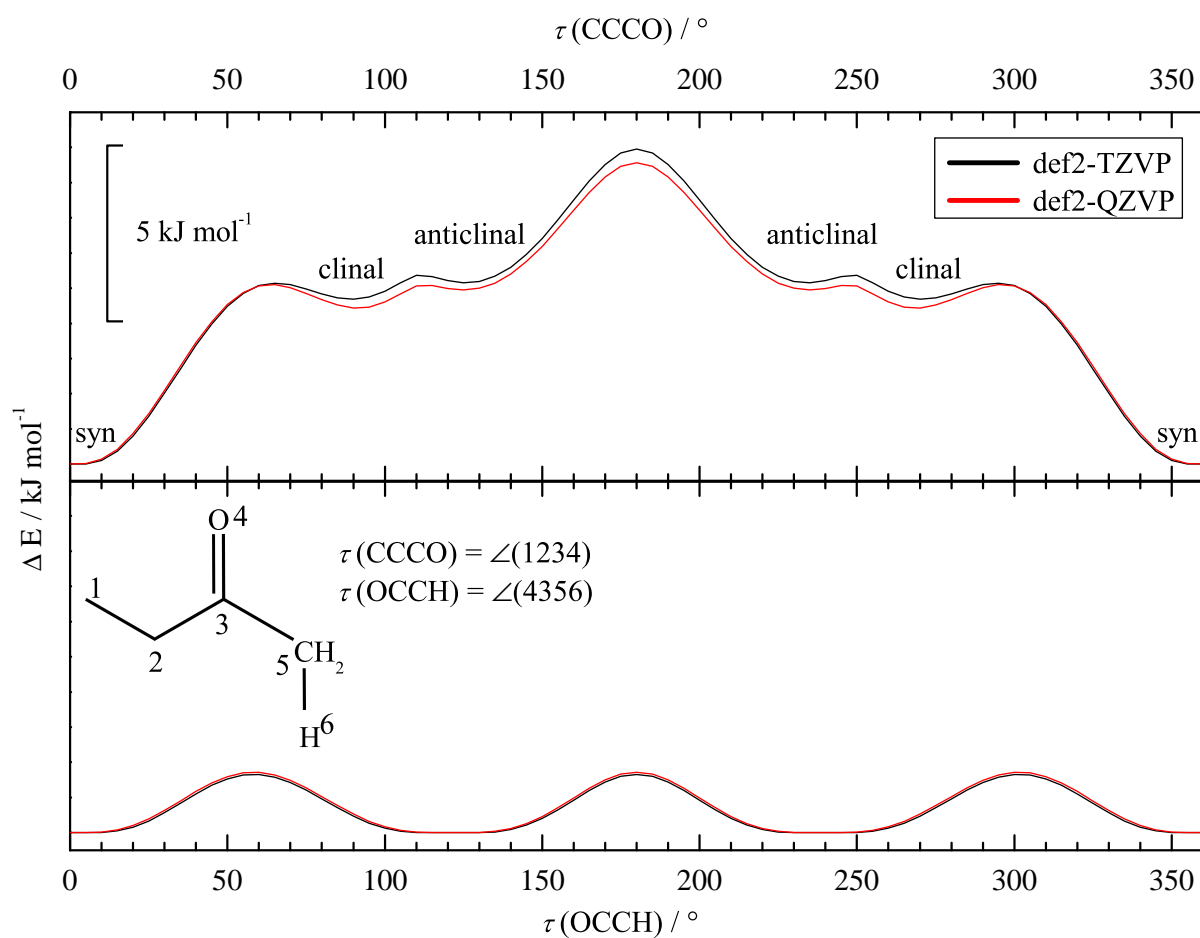


Fig. S2: Relaxed B3LYP-D3(BJ,ABC) scans with def2-TZVP and def2-QZVP along the CCCO (upper panel) torsional angle τ (with pairs of equivalent clinal minima at 90° , 270° and anti-clinal minima at 125° , 235° , respectively) and aliphatic OCCH (lower panel) torsional angle τ for methyl-ethyl-ketone (MEK) in syn configuration (with equivalent minima at 0° , 120° , 240°). In jet expansions, barriers below about 5 kJ mol^{-1} (see insert for the scale) can be overcome. MEK is thus expected to relax quantitatively into the syn conformation in a jet expansion.

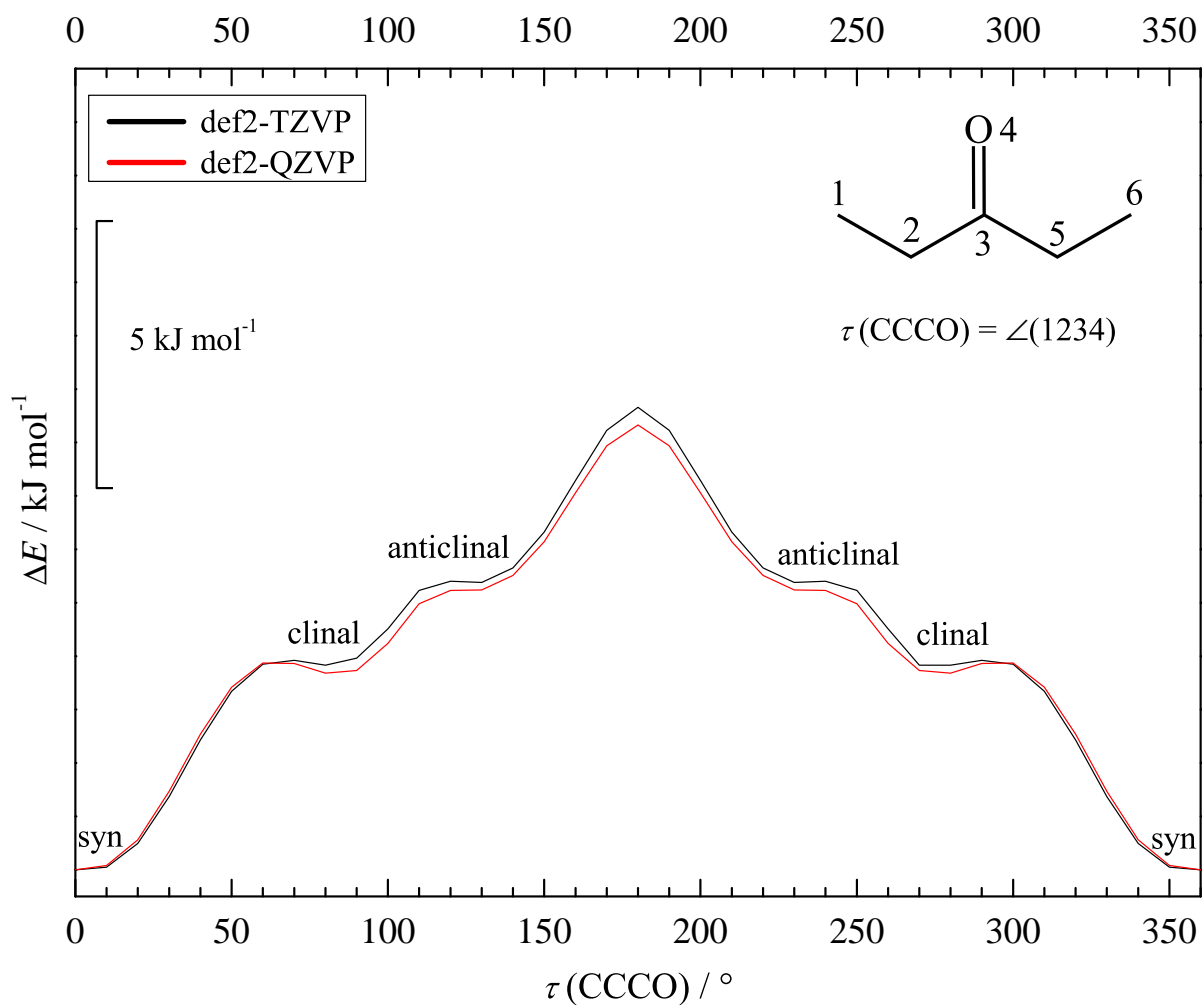


Fig. S3: Relaxed B3LYP-D3(BJ,ABC)/def2-TZVP scan along one alkylic CCCO torsional angle τ for ethyl-ethyl-ketone EEK (with shallow secondary minima at 80° , 130°). Barriers below 5 kJ mol^{-1} (see insert for scale) can be largely overcome in a jet expansion and relax into the most stable isomer (at 0°). EEK monomer is thus expected to relax completely into the syn conformation in a jet expansion.

1.2 Dimers

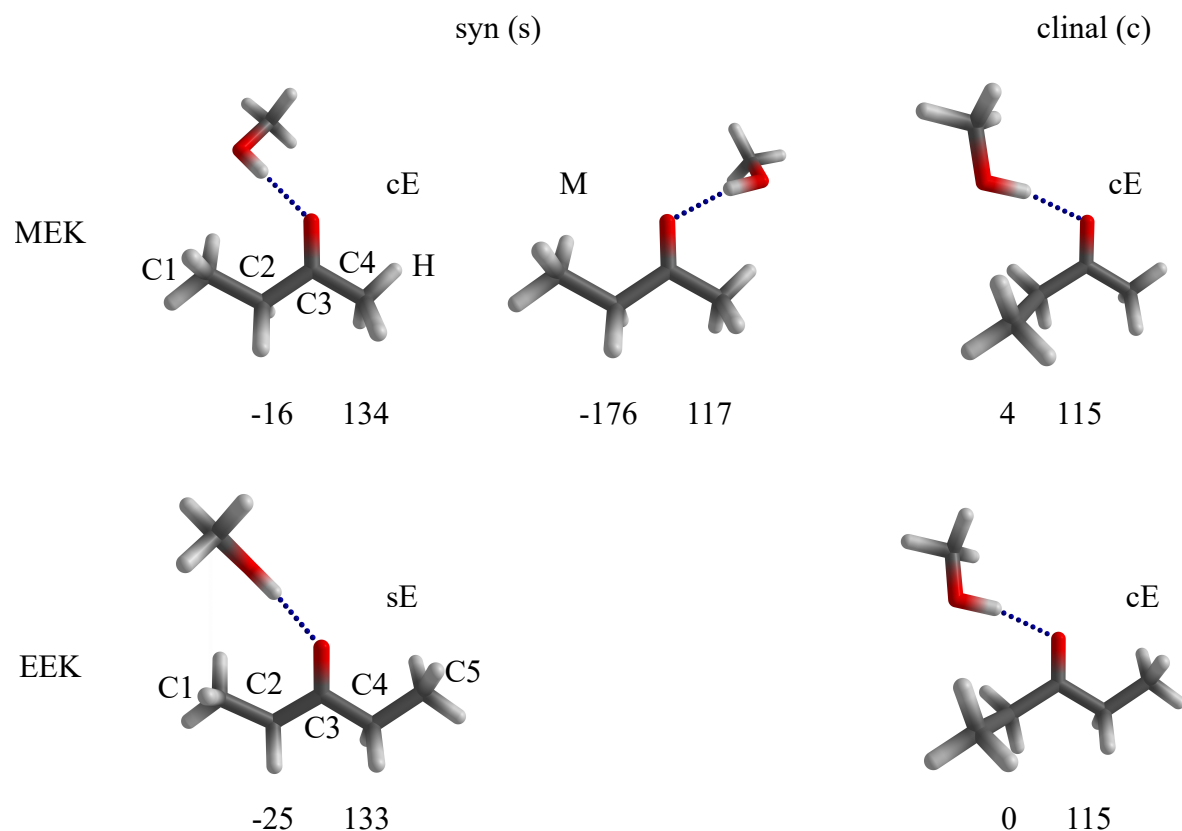


Fig. S4: Structures of the two most stable E-docking 1:1 clusters (syn energetically below clinal) of methyl-ethyl-ketone (MEK) and ethyl-ethyl-ketone (EEK) with MeOH at B3LYP-D3(BJ,ABC)/def2-TZVP level (naming after Newman Projection (NP))^{S5}. Also shown is the most stable M-docking MEK isomer. Below the structures, the hydrogen bond torsional angle τ (C2-C3=O \cdots H, negative when the hydrogen bond points away from the reader) and the hydrogen bond angle α (C3=O \cdots H) are given in $^\circ$ in this sequence. For methyl side docking (M) and clinal ethyl side docking (E), α is slightly below 120° and the torsion out of the carbonyl plane is minor. For syn ethyl side docking, α is above 120° and the out-of-plane torsion is larger, geometrically indicating steric strain for the coplanar arrangement of the methanol OH with the ketone scaffold.

Tab. S3: Weak method-dependence of the hydrogen bond angles α and τ from Fig. S4 together with the alkyl torsional angles τ_l (O=C3C2C1) and τ_r (O=C3C4H/C5) in the 1:1 complex, all in $^\circ$.

Ketone	NP	Method	τ_l/τ_r	E			M		
				α	τ	τ_l/τ_r	α	τ	
MEK	syn	B3LYP-D3	8/-14	134	-16	6/-16	117	-176	
	clinal		83/8	115	4	-	-	-	
MEK	syn	X3LYP-D3	8/-13	133	-16	6/-16	115	-176	
	clinal		83/8	113	4	-	-	-	
MEK	syn	X3LYP	9/-13	137	-15	6/-17	118	-175	
	clinal		83/8	117	3	-	-	-	
EEK	syn	B3LYP-D3	15/-10	133	-25	-	-	-	
	clinal		79/5	115	0	-	-	-	
EEK	syn	X3LYP-D3	16/-10	132	-24	-	-	-	
	clinal		79/5	114	1	-	-	-	
EEK	syn	X3LYP	18/-9	135	-26	-	-	-	
	clinal		77/5	118	2	-	-	-	

Tab. S4: Docking preference of methanol complexes for methyl-ethyl-ketone (MEK) or ethyl-ethyl-ketone (EEK) predicted by B3LYP, X3LYP and BP86 with and (for X3LYP also) without D3(BJ) correction in kJ mol^{-1} relative to the syn(s)-ethyl(E)-sided structure. ΔE^0 includes the harmonically approximated zero-point energy and ΔE^{el} excludes it. Positive values indicate a higher stability for s-docking, as compared to docking to the c(linal) conformation of an E(thyl group) or M-docking in the case of MEK. The negative c-s differences for the dispersion corrections $\Delta^{\text{el}}\text{D3}$ and $\Delta^0\text{D3}$ show that dispersion favors c over s, but this is more than compensated by total zero-point energy effects, such that the sE conformation is the direct competitor to M-docking (for MEK) or winner (for EEK) in the case of methanol. The tight outcome of the s-c competition for EEK suggests that more bulky alcohols may instead stabilise c-conformations. BP86 predicts a significantly more stable M conformation, but otherwise the three methods perform rather similarly.

Ketone	Method	With D3		Without D3		$\Delta^{\text{el}}\text{D3}$	$\Delta^0\text{D3}$
		ΔE^{el}	ΔE^0	ΔE^{el}	ΔE^0		
MEK	B3LYP M-sE	-2.81	-2.27	-	-	-	-
	B3LYP cE-sE	-0.01	+1.29	-	-	-	-
MEK	X3LYP M-sE	-2.91	-2.48	-3.03	-2.43	+0.12	-0.05
	X3LYP cE-sE	-0.66	+0.71	+1.40	+2.69	-2.06	-1.99
MEK	BP86 M-sE	-3.82	-3.44	-	-	-	-
	BP86 cE-sE	-0.36	+0.69	-	-	-	-
EEK	B3LYP cE-sE	-0.29	+0.47	-	-	-	-
	X3LYP cE-sE	-0.54	+0.07	+0.50	+1.39	-1.04	-1.33
EEK	BP86 cE-sE	-0.51	+0.22	-	-	-	-

Tab. S5: Docking effect on the harmonic OH stretching wavenumbers ω and resulting wavenumber shifts $\Delta\omega$ (in cm^{-1}) for docking variants of methanol complexes with methyl-ethyl-ketone (MEK) or ethyl-ethyl-ketone (EEK). The wavenumber shifts refer to syn-ethyl(sE)-docking (which is always the most upshifted variant) relative to alternatives clinal-ethyl(cE) and methyl(M). The large spectral effects indicate that experiment can easily discriminate between sE and cE docking. The corresponding harmonic OH stretching wavenumber of the methanol monomer is 3810 cm^{-1} for B3LYP-D3, 3820 cm^{-1} for X3LYP-D3 and 3819 cm^{-1} for X3LYP.

Ketone	Method	ω_M	ω_{sE}	ω_{cE}	$\Delta\omega_{sE-M}$	$\Delta\omega_{sE-cE}$
MEK	B3LYP-D3(BJ)	3620	3670	3604	+51	+67
	X3LYP-D3(BJ)	3618	3670	3601	+52	+68
	X3LYP	3639	3691	3628	+52	+62
EEK	B3LYP-D3(BJ)	-	3666	3599	-	+66
	X3LYP-D3(BJ)	-	3665	3597	-	+69
	X3LYP	-	3686	3626	-	+60

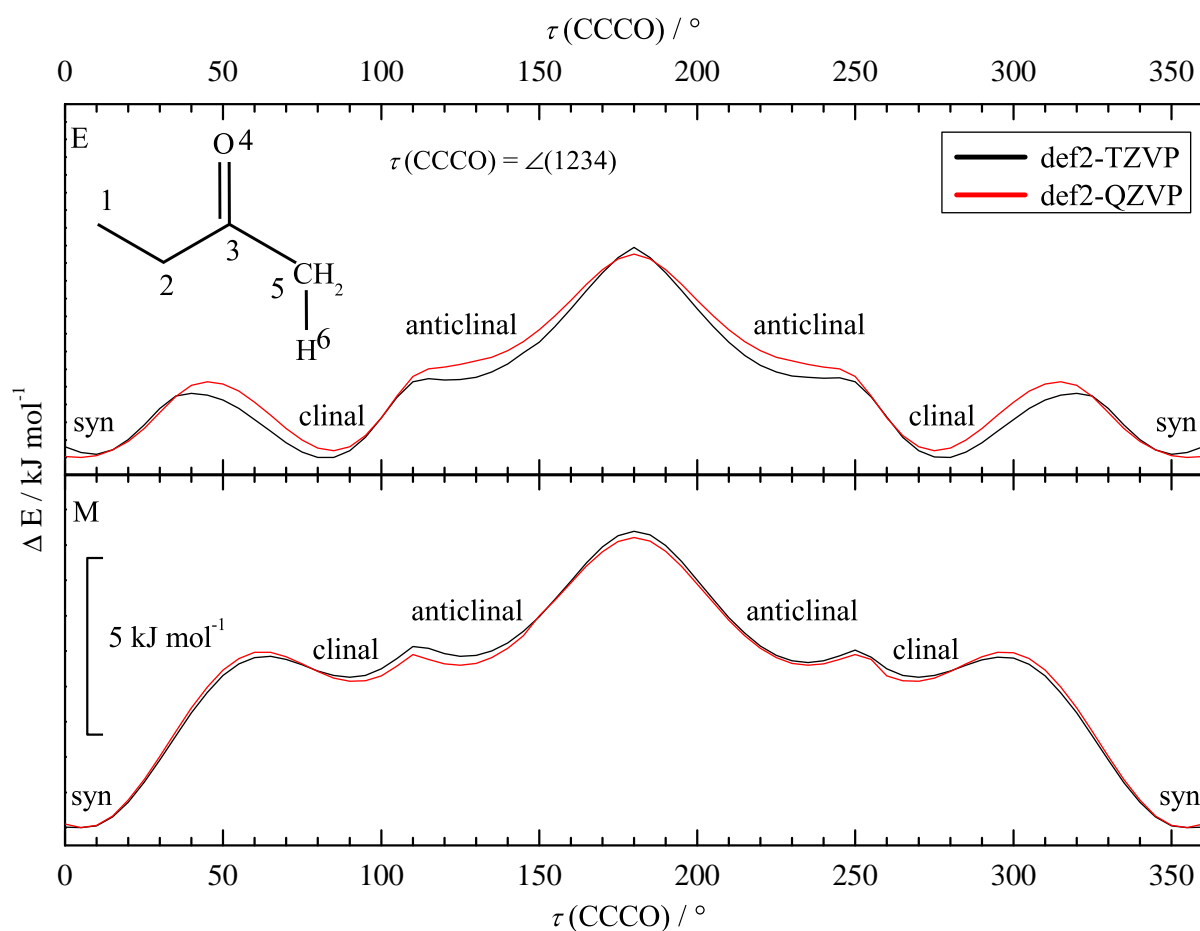


Fig. S5: Relaxed MEK B3LYP-D3(BJ,ABC) scans with def2-TZVP and def2-QZVP along the CCCO torsional angle τ for ethyl docking (E, upper panel, with equivalent minima at 10° , 350° and 80° , 280° as well as 120° , 240°) and methyl-docking (M, lower panel, with equivalent minima at 10° , 350° and 90° , 270° as well as 130° , 230°) of MeOH. In jet expansions, barriers below about 5 kJ mol^{-1} (see insert for the scale) can be overcome and in the case of M-docking relax into the most stable syn isomer. For E-docking, the clinal conformation is electronically slightly more stable than syn.

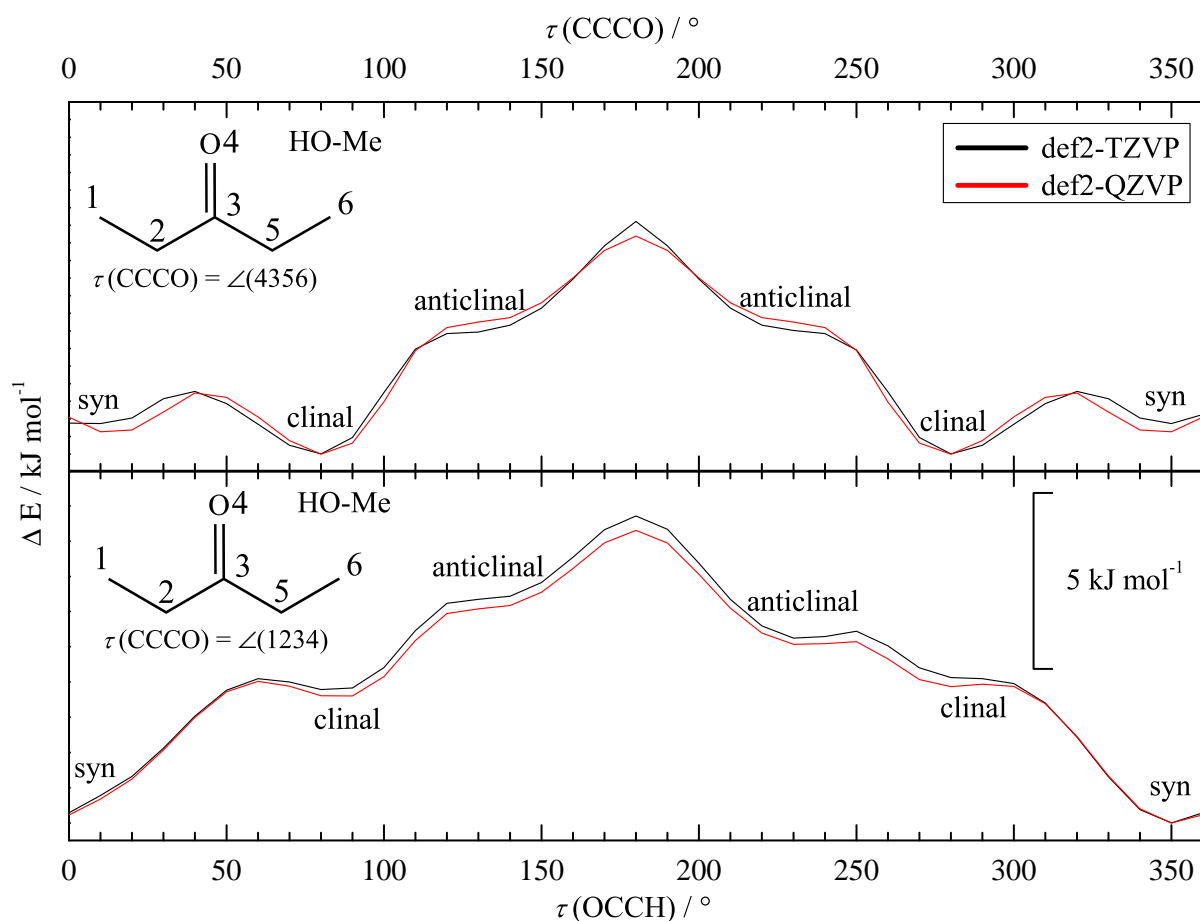


Fig. S6: Relaxed EEK B3LYP-D3(BJ,ABC) scans with def2-TZVP and def2-QZVP along the CCCO torsional angle τ (with equivalent minima at 20° , 340° and 80° , 280°) on the methanol (MeOH) docking side (upper panel) and the CCCO torsional angle τ on the opposite methanol docking side (lower panel) for dimers of ethyl-ethyl-ketone with MeOH. In jet expansions, barriers below about 5 kJ mol^{-1} (see insert for the scale) can be overcome and, in the case of torsion on the opposite docking side (lower panel), relax into the most stable syn conformation. For torsion on the docking side (upper panel), the clinal conformation slightly wins over the syn conformation before taking zero point energy effects into account.

Tab. S6: Calculated infrared band strengths σ in km mol^{-1} for each MeOH docking side in methyl-ethyl-ketone (MEK) or ethyl-ethyl-ketone (EEK) and corresponding infrared band strength ratios $\frac{\sigma_i}{\sigma_j}$ ($i, j = \text{M, sE, cE}$, see Tab. S5). Within the expected accuracy of these harmonic predictions, the visibility of all competing isomers is the same, such that the spectrum closely reflects abundance.

Ketone	Method	σ_{M}	σ_{sE}	σ_{cE}	$\frac{\sigma_{\text{sE}}}{\sigma_{\text{M}}}$	$\frac{\sigma_{\text{cE}}}{\sigma_{\text{M}}}$	$\frac{\sigma_{\text{cE}}}{\sigma_{\text{sE}}}$
MEK	B3LYP-D3(BJ)	601	540	615	0.899	1.023	1.138
	X3LYP-D3(BJ)	636	575	642	0.904	1.010	1.117
	X3LYP	587	511	585	0.871	0.997	1.145
	BP86-D3(BJ)	705	570	727	0.809	1.031	1.275
EEK	B3LYP-D3(BJ)	-	532	652	-	-	1.227
	X3LYP-D3(BJ)	-	563	682	-	-	1.212
	X3LYP	-	522	617	-	-	1.182
	BP86-D3(BJ)	-	622	757	-	-	1.217

Tab. S7: LED analysis in kJ mol^{-1} comparing dispersion contributions for the methyl(M)- or clinal ethyl (cE) vs. the syn ethyl(sE)-docking of MeOH at DLPNO-CCSD(T) level for the B3LYP-D3(BJ)/def2-TZVP optimised minimum structures of methyl-ethyl-ketone (MEK) or ethyl-ethyl-ketone (EEK). ΔE^{el} is the full CCSD(T) energy difference and $\Delta E_{-D}^{\text{el}}$ is the difference after subtraction of the dispersion contribution. The interfragment dispersion contributions of strong and weak pairs, as displayed in the ORCA LED output, were combined to yield the total dispersion contribution to the intermolecular interaction within the LED scheme. ΔD in the last column gives the dispersion correction advantage for syn ethyl-docking. A positive value means that the sE-docking structure offers more dispersion attraction than the corresponding cE- or M-docking structure. For reference, the corresponding DFT-D3 energies ΔE^{el} (see Tab. S4) are also given in the first number column. The numbers suggest that M-docking stability is overestimated by DFT, independent on dispersion, and that cE may profit in a somewhat unsystematic way (more in MEK than in EEK) from dispersion.

Ketone	pre-opt. level		DFT-D3	DLPNO -	CCSD(T)	ΔD	
			ΔE^{el}	ΔE^{el}	$\Delta E_{-D}^{\text{el}}$		
MEK	B3LYP-D3(BJ)	M-sE	-2.81	-1.55	-1.37	-0.19	
		X3LYP-D3(BJ)	M-sE	-2.91	-1.54	-1.42	-0.12
		BP86-D3(BJ)	M-sE	-3.82	-1.97	-2.21	+0.24
	B3LYP-D3(BJ)	cE-sE	-0.01	+0.55	+2.30	-1.75	
		X3LYP-D3(BJ)	cE-sE	-0.66	+0.49	+2.73	-2.24
		BP86-D3(BJ)	cE-sE	-0.36	-0.17	+1.48	-1.65
EEK	B3LYP-D3(BJ)	cE-sE	-0.29	-0.51	+0.15	-0.66	
		X3LYP-D3(BJ)	cE-sE	-0.54	-0.58	-0.60	+0.02
		BP86-D3(BJ)	cE-sE	-0.51	-0.50	+0.13	-0.62

2 Experimental Results

Tab. S8: Experimental OH stretching wavenumbers $\tilde{\nu}$ and resulting wavenumber shifts $\Delta\tilde{\nu}_{h-1}$ for high (h) and low (l) lying spectral signals for methyl-ethyl-ketone (MEK) or ethyl-ethyl-ketone (EEK) and MeOH 1:1 complexes in cm^{-1} . Additionally, given is $\tilde{\nu}$ for the 1:1 complex of MeOH with the symmetric methyl-methyl-ketone (MMK, acetone) taken from the literature.^{S6} The numbers suggest a purely experimental, robust increment pattern, where M-to-E substitution on the remote side lowers the MeOH wavenumber by about 3 cm^{-1} (likely an inductive effect on the C=O group) and the spectral splitting due to the direct interaction (likely an interplay of strain and attraction due to the extra CH_2 group) is an order of magnitude larger.

Ketone	$\tilde{\nu}$		$\Delta\tilde{\nu}_{h-1}$
	high	low	
MEK	3574	3527	47
EEK	3572	-	-
MMK	-	3530	-

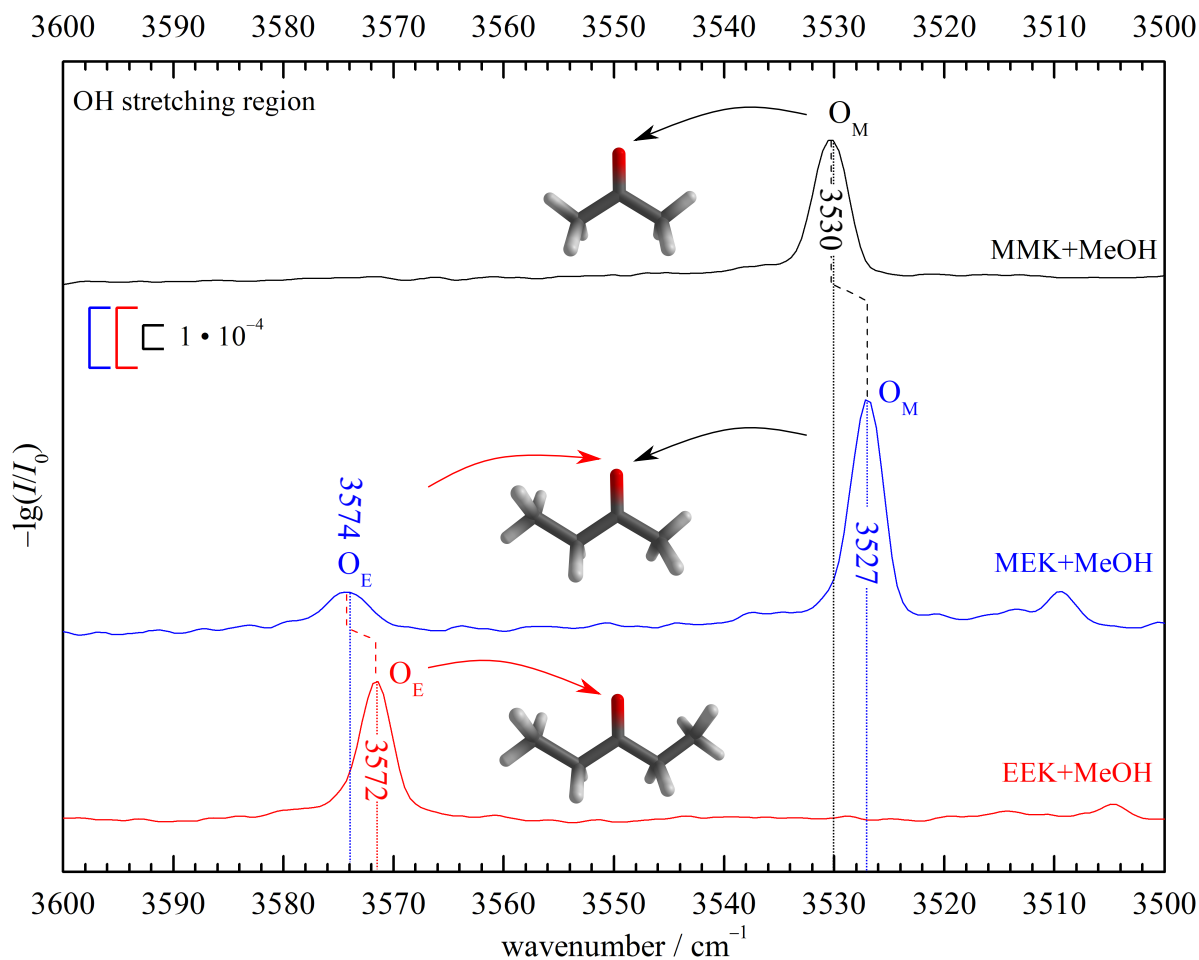


Fig. S7: Comparison between FTIR jet OH stretching spectra of MEK, EEK and MMK (methyl-methyl-ketone or acetone) with MeOH. The black spectrum^{S6} was scaled to match the O_M signal intensity for better comparison. OH stretching signals of complexes with the symmetric ketones EEK and MMK are connected to the corresponding signals in the asymmetric MEK+MeOH spectrum by dashed lines. The similarities between O_M and O_E signals support the isomer assignment in MEK+MeOH. The experimental wavenumbers of the band maxima (see also Tab. S8) are indicated.

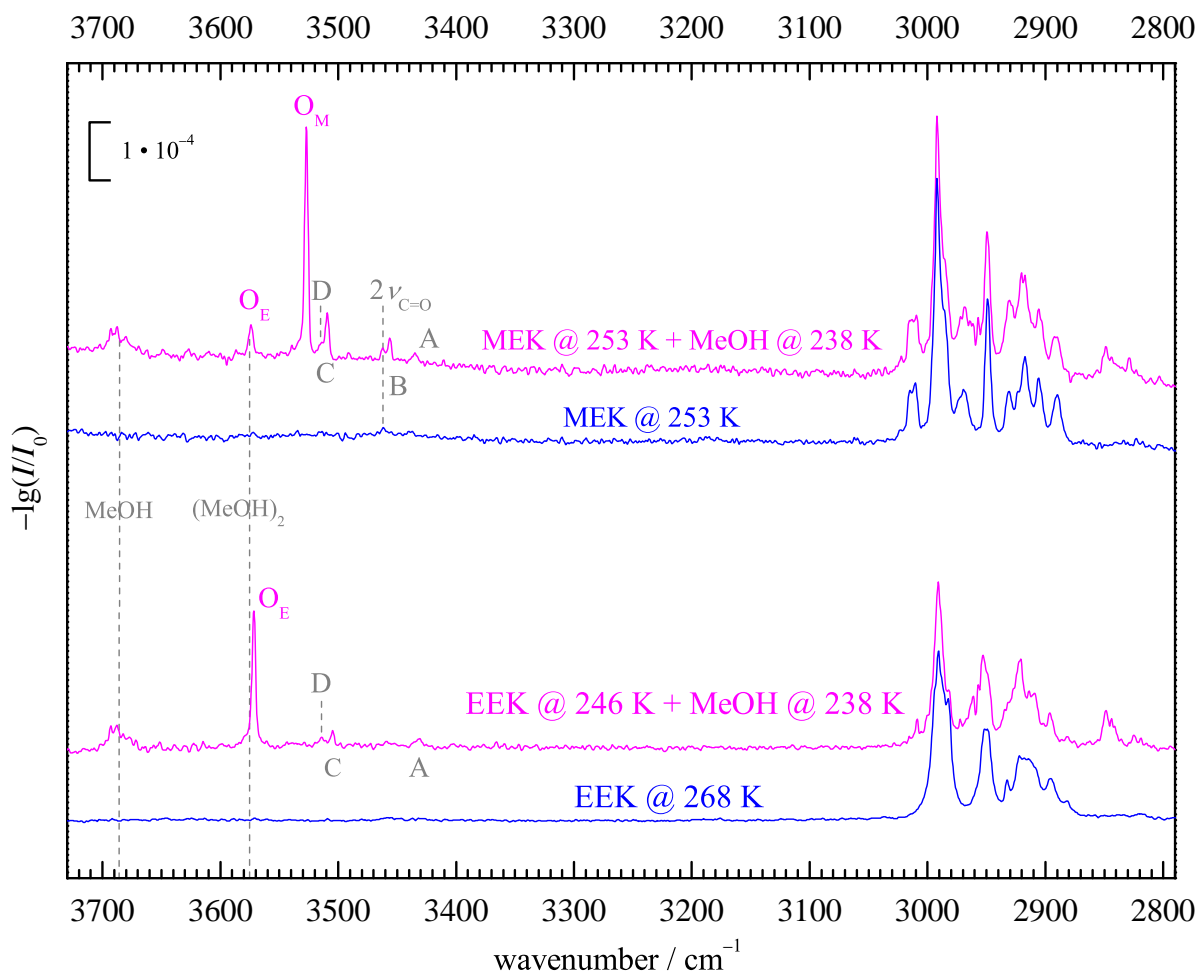


Fig. S8: FTIR jet OH stretching spectra of MEK and EEK with MeOH compared to corresponding (monomer-scaled) pure ketone spectra (blue) taken at 0.75 bar stagnation pressure. For the MEK+MeOH spectrum, the immediate pre-pulse scan was used for background correction with better atmospheric water compensation, for the others, the earlier block of reference scans was used for better signal-to-noise ratio. The position of the weak C=O overtone around 3462 cm^{-1} is marked with $2\nu_{\text{C=O}}$ and a dashed line. Further dashed lines mark MeOH and $(\text{MeOH})_2$. In contrast to MEK, EEK $2\nu_{\text{C=O}}$ contributions are comparable to the noise level.

2.1 Methyl-ethyl-ketone (MEK) + MeOH

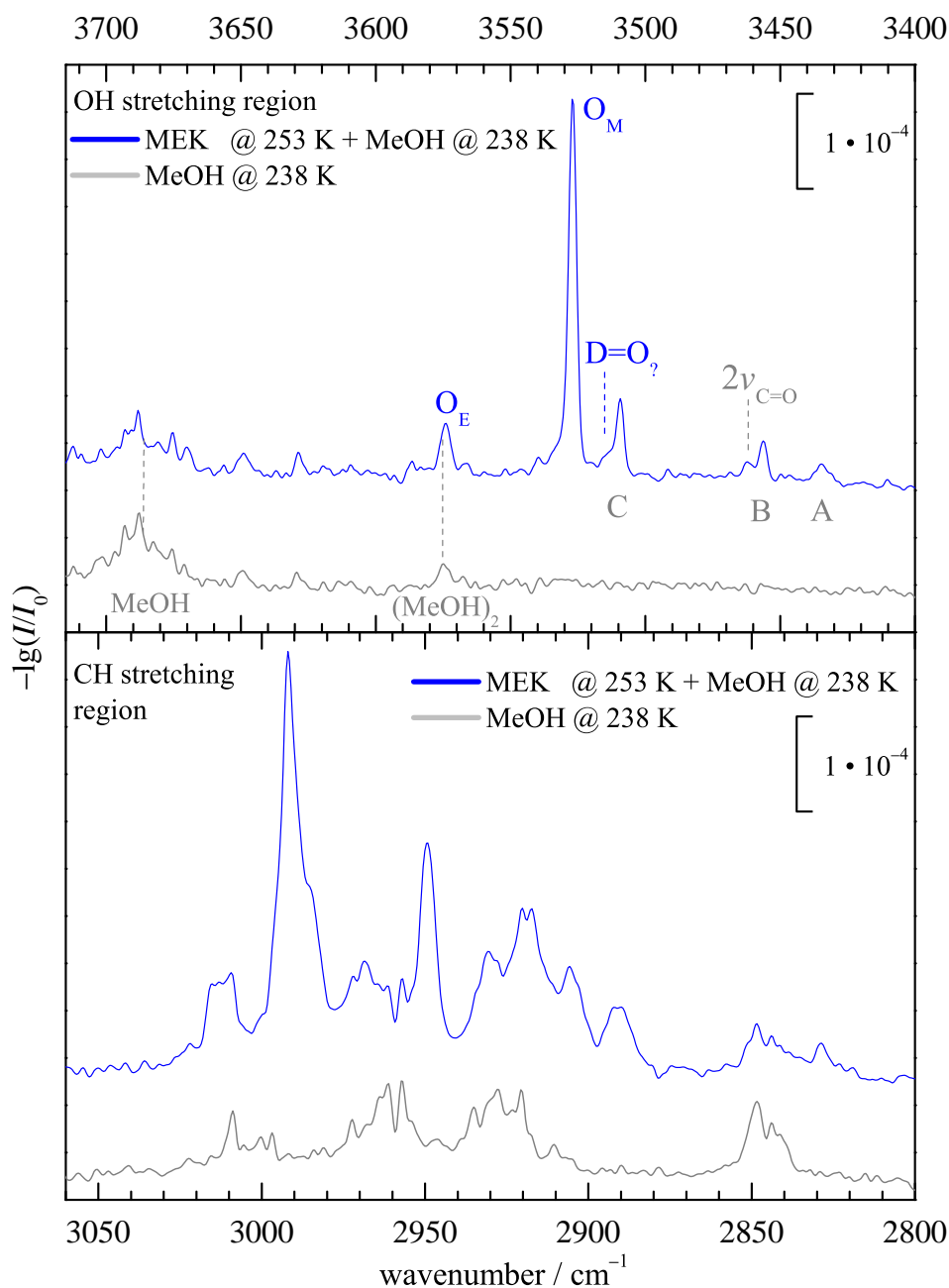


Fig. S9: OH stretching spectrum of MEK with methanol (upper panel) in comparison to pure methanol, recorded under the same helium supersonic jet conditions at a stagnation pressure of 0.75 bar. The $(\text{MeOH})_2$ signal overlaps with the O_E signal assigned to an isomer of the 1:1 complex, but is expected to be close to the noise level in the mixed spectrum. Most of the intensity is thus due to the 1:1 isomer, but the O_M signal (ca. 3 cm^{-1} FWHM) due to another 1:1 isomer clearly dominates. For a potential minor third 1:1 contribution $\text{D} = \text{O}_?$, see the main text. $2\nu_{\text{C}=\text{O}}$ marks the position of the C=O overtone wavenumber (see Fig. S8). Other cluster compositions (A,B,C) can be observed (see Fig. S10 and S11). For comparison, the CH stretching region (lower panel) is also shown.

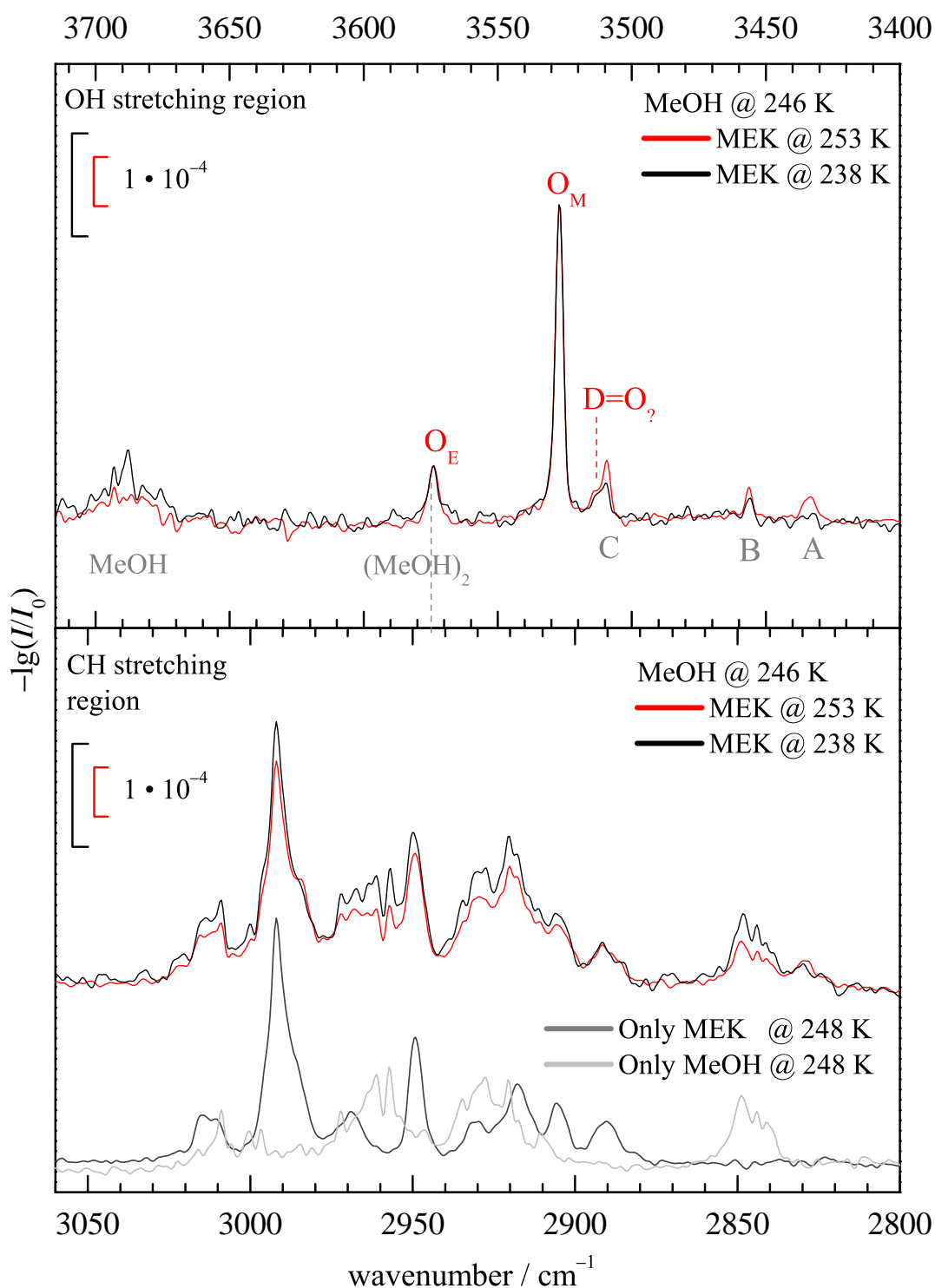


Fig. S10: FTIR jet OH stretching spectra of methanol (upper panel) in the presence of different MEK concentrations, taken at 0.75 bar stagnation pressure and scaled to match the 1:1 complex O_M signal intensity. The same scaling is shared by O_E and perhaps $D = O_2$. Signals A and C clearly involve more MEK in their cluster stoichiometry, for B this is unclear. In the lower panel, the CH stretching region of the scaled spectra and the two pure substance spectra (MEK and MeOH only) are shown, to confirm that more MeOH is needed to compensate less MEK for the same 1:1 cluster scaling.

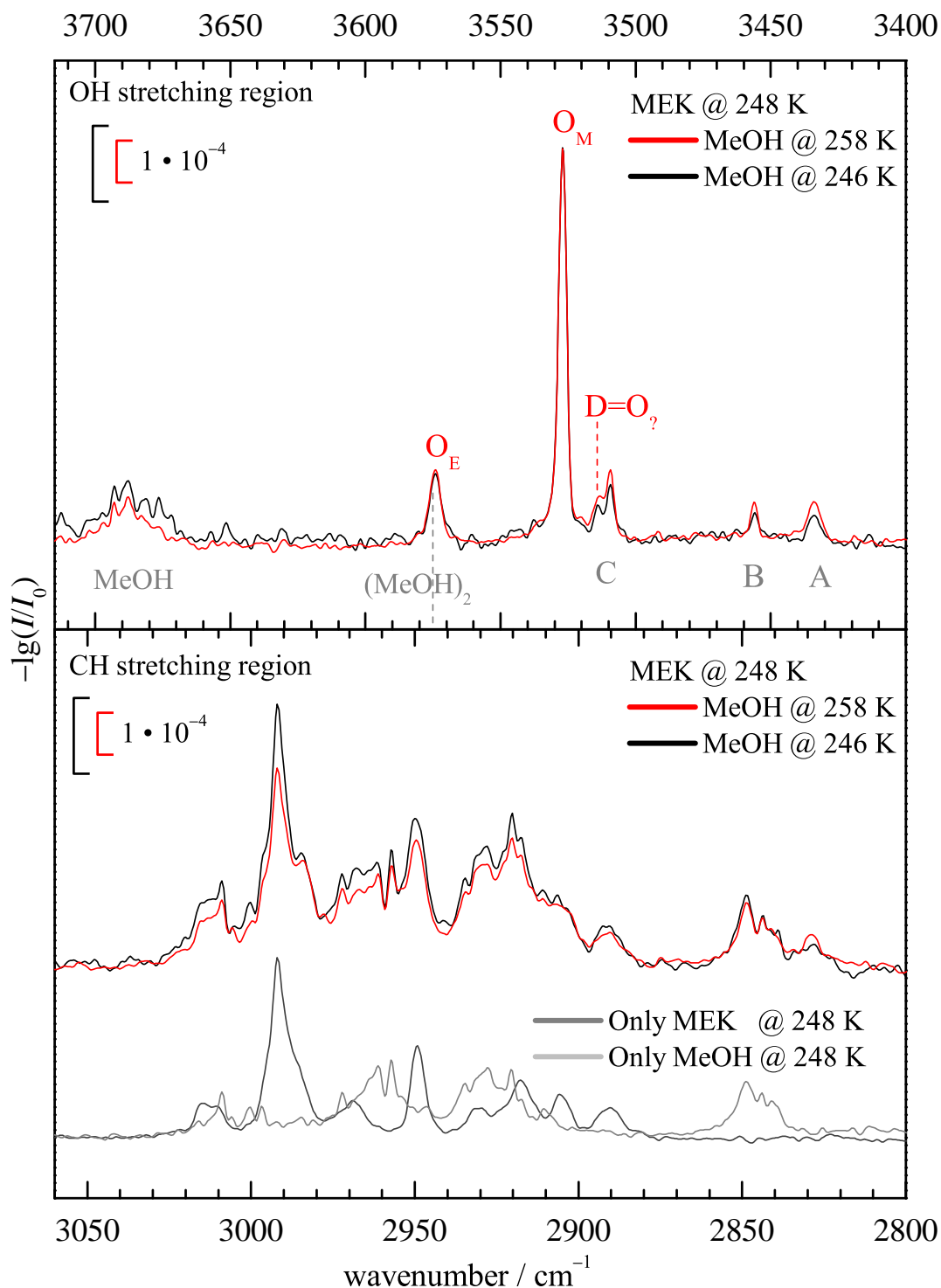


Fig. S11: FTIR jet OH stretching spectra of MEK (upper panel) in the presence of different methanol concentrations, taken at 0.75 bar stagnation pressure and scaled to match the 1:1 complex O_M signal intensity. The same scaling is shared by O_E . For the black spectrum, the pre-scan was used for background compensation with better atmospheric water cancellation. Signals A, B, C, $D = O?$ clearly involve more methanol in their cluster stoichiometry. In the lower panel, the CH stretching region of the scaled spectra and the two pure substance spectra (MEK and MeOH only) are shown, to confirm that more MEK is needed to compensate less MeOH for the same 1:1 cluster scaling.

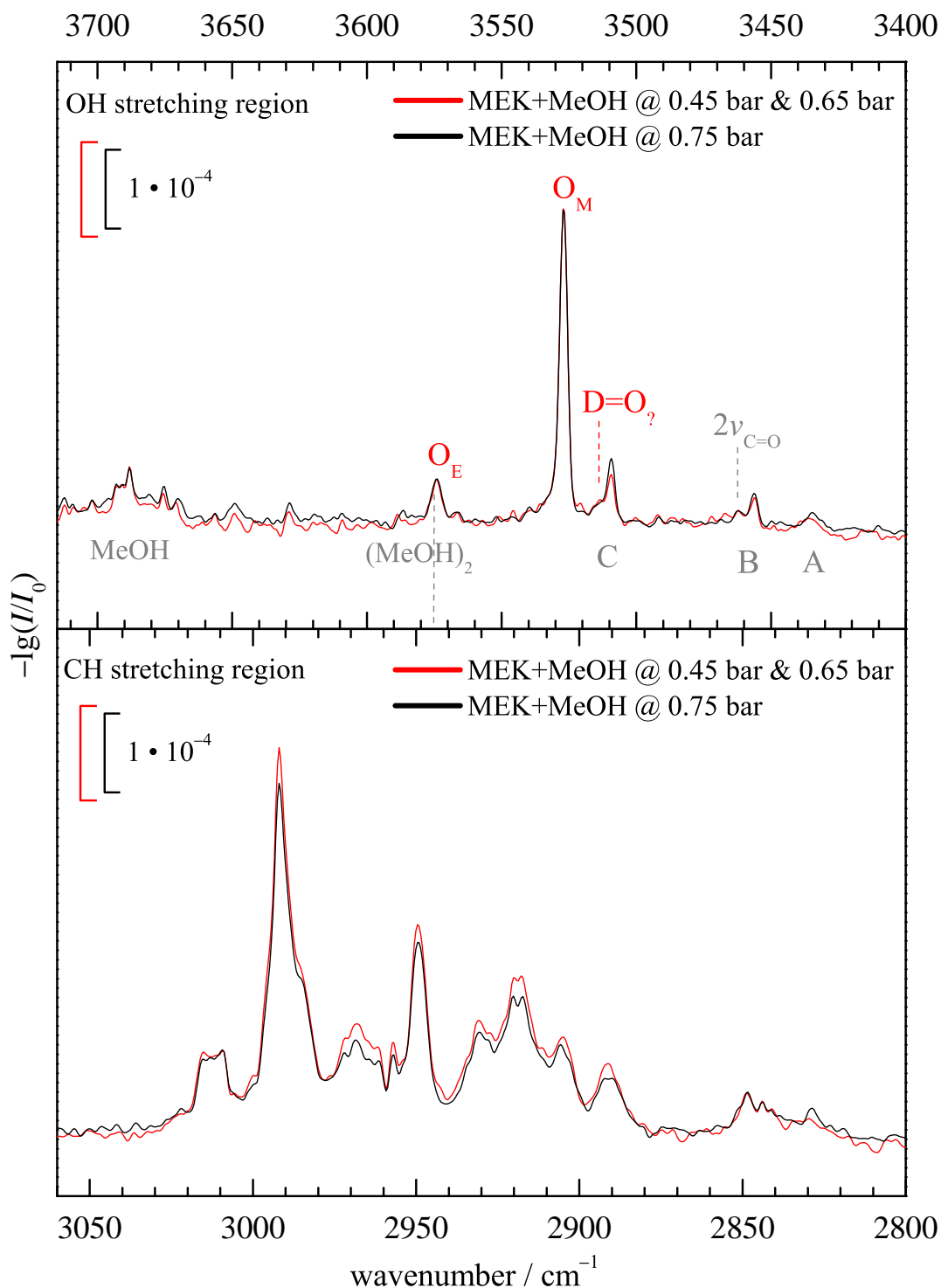


Fig. S12: FTIR jet spectra of MEK (upper panel) with methanol taken at the same concentration ratio (MEK @ 253 K and MeOH @ 238 K) but different stagnation pressures, which influence the efficiency of collisional cooling in the jet expansion. The spectra are scaled to match the 1:1 complex O_M signal intensity. Due to similar scaling behavior, the spectra taken at 0.45 bar and 0.65 bar were averaged before scaling to obtain the red spectrum. O_E (and perhaps also $D = O_?$) is seen to scale like O_M . The signal C clearly deviates in its scaling behaviour, supporting its different cluster stoichiometry. The lower panel shows that the 1:1 scaled CH stretching region shrinks slightly with increasing pressure, as it should if the expansion is monomer-dominated.

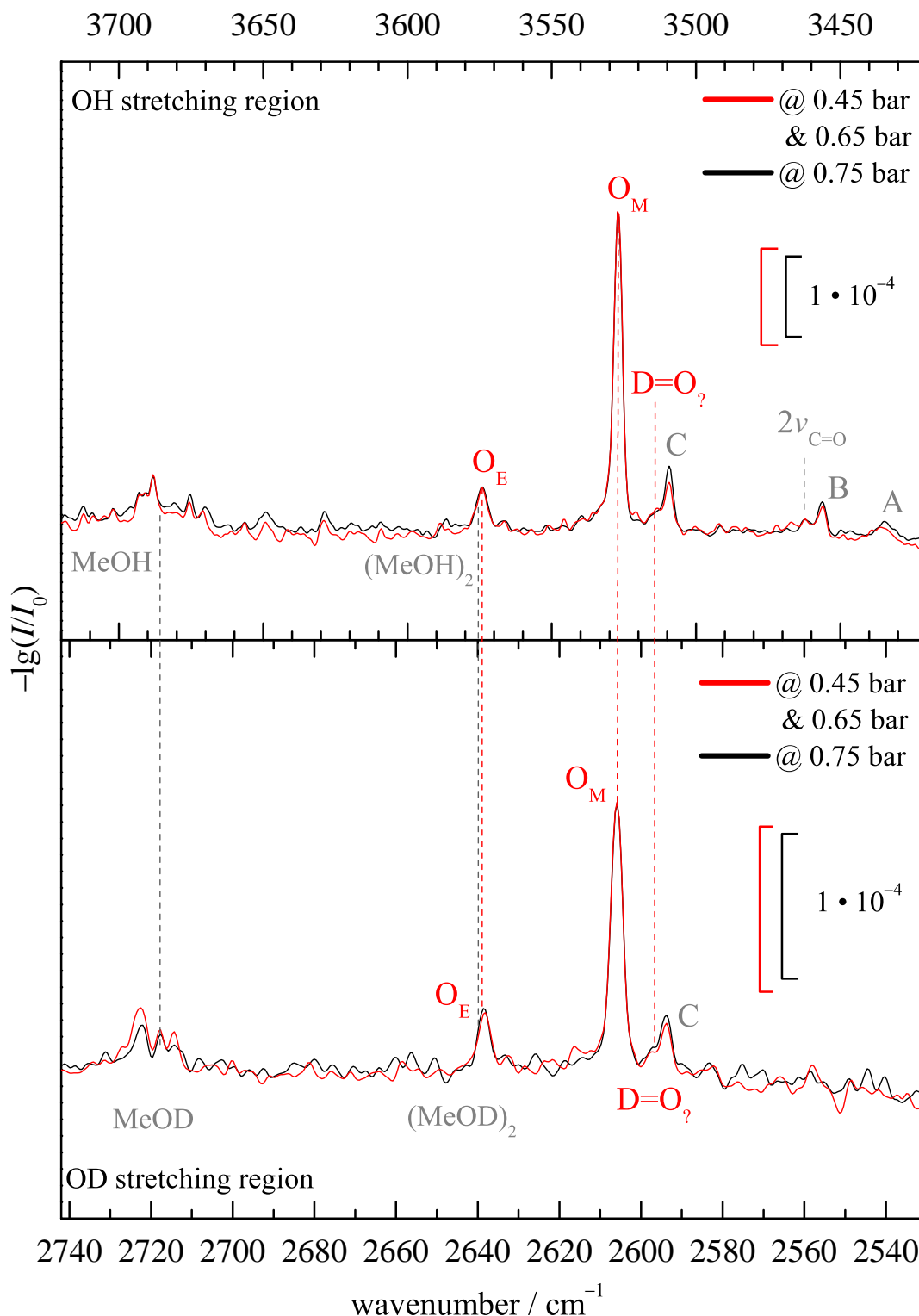


Fig. S13: Comparison of the spectra for MEK with MeOH (upper panel, see Fig. S12) and MeOD (lower panel) taken at the same conditions (MEK @ 253 K and MeOH @ 238 K) with different stagnation pressures, after stretching the OD wavenumber axis with $\sqrt{2}$ and matching the two monomer transitions 3686 cm^{-1} and 2718 cm^{-1} .^{S7} Due to their similarity, the spectra taken at 0.45 bar and 0.65 bar were averaged prior to scaling giving the red spectrum for both isotopologues. The pattern remains essentially unchanged upon isotope substitution (vertical red dashed lines), suggesting that the O-peaks (at least the stronger O_M and O_E signals) are not due to some resonance but rather due to different isomers of the 1:1 complex. However, the decreased dominance of O_M upon deuteration does not fit the expectation for an O_M-weakening zero point energy effect, see Tab. S4.

2.2 Ethyl-ethyl-ketone (EEK) + MeOH

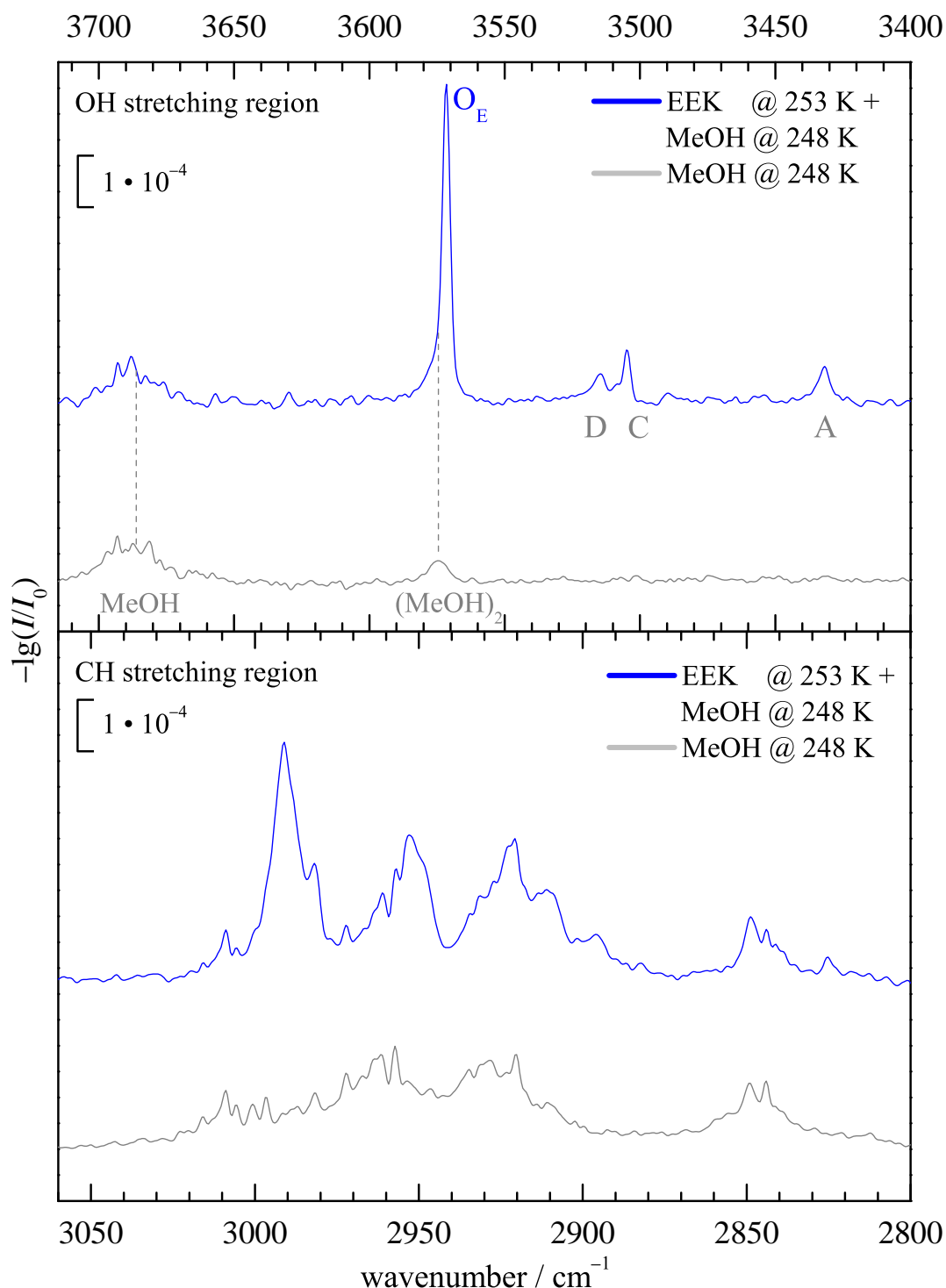


Fig. S14: FTIR jet OH stretching spectrum of EEK with methanol (upper panel) in comparison to pure methanol taken at the same conditions with a stagnation pressure of 0.75 bar. The dimer $(\text{MeOH})_2$ partially overlaps with the assigned 1:1 complex O_E (less so than for MEK), but the contribution from $(\text{MeOH})_2$ is close to the noise level in the mixed spectrum. For comparison the CH stretching region (lower panel) is also shown.

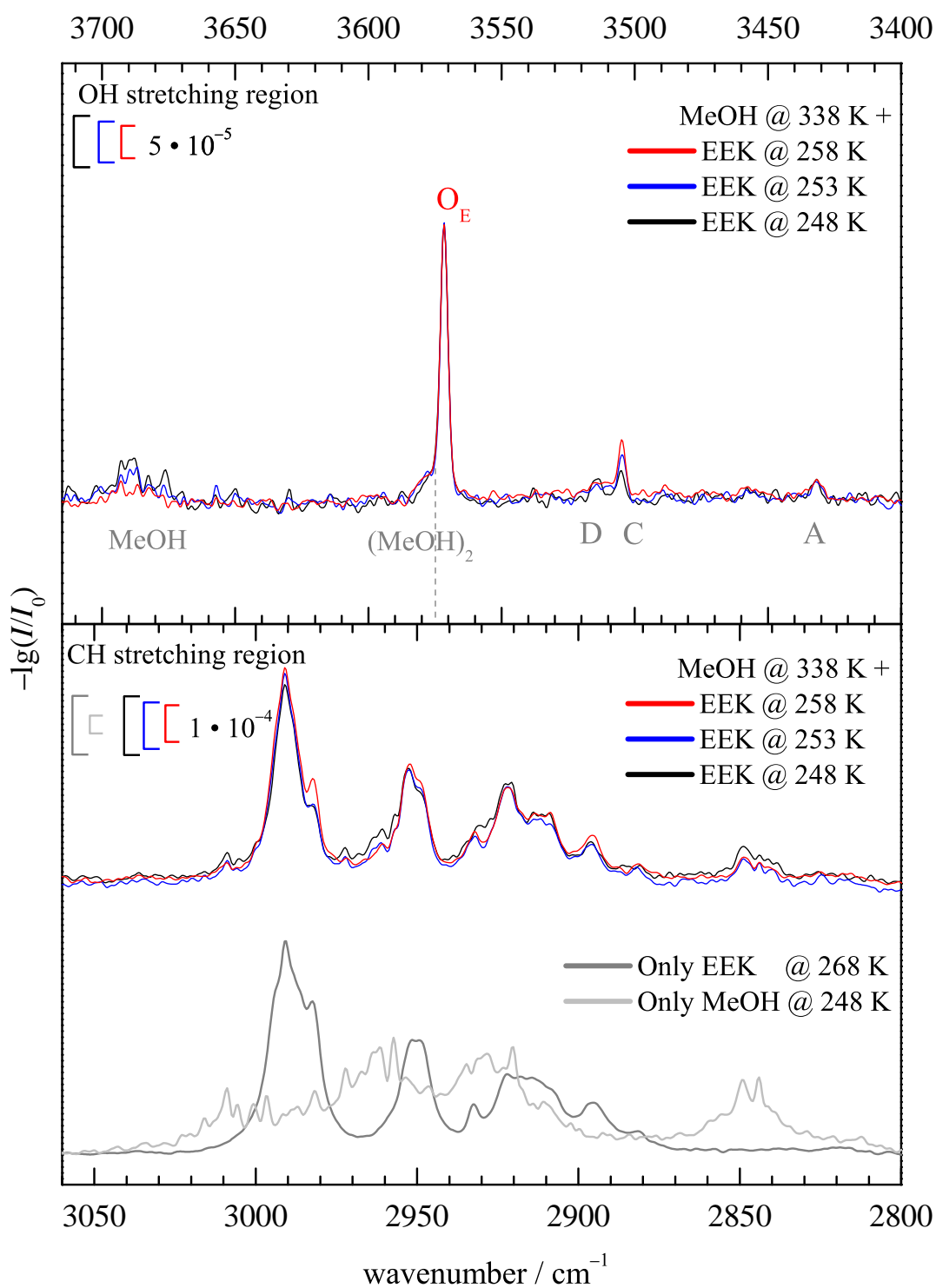


Fig. S15: FTIR jet OH stretching spectra of methanol (upper panel) in the presence of different EEK concentrations, taken at 0.75 bar stagnation pressure and scaled to match the 1:1 complex O_E signal intensity. Among the other signals, C is clearly due to another cluster composition. In the lower panel, the CH stretching region of the scaled spectra and the two pure substance spectra (EEK and MeOH only) show that more methanol is needed to compensate for a decreasing EEK concentration in the scaled spectra, confirming the mixed cluster origin of the matched OH signals.

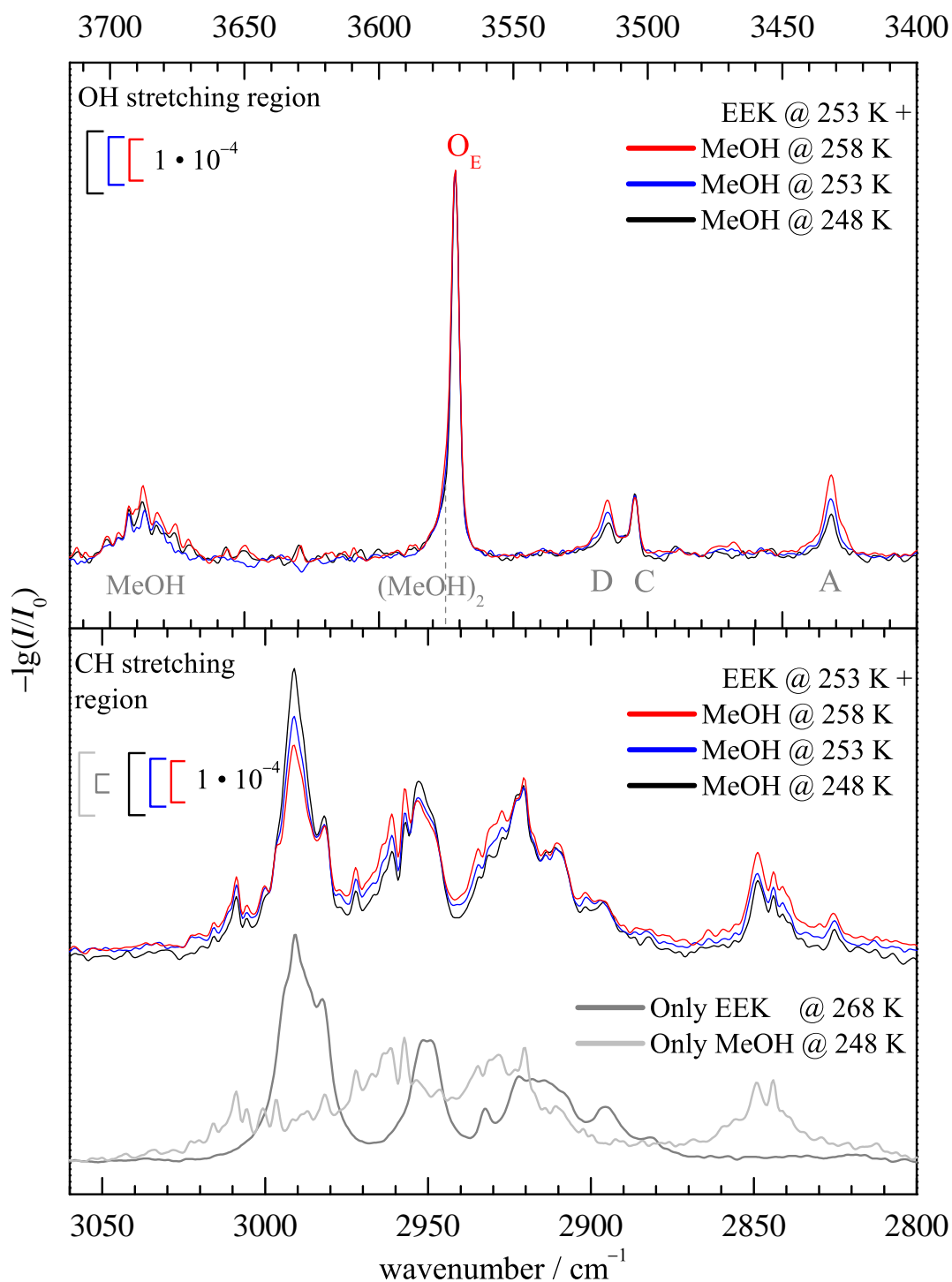


Fig. S16: FTIR jet OH stretching spectra of EEK (upper panel) in the presence of different MeOH concentrations, taken at 0.75 bar stagnation pressure and scaled to match the 1:1 complex O_E signal intensity. Among the other signals, A and D are clearly due to another cluster composition. In the lower panel, the CH stretching region of the scaled spectra and the two pure substance spectra (EEK and MeOH only) show that more EEK is needed to compensate for a decreasing methanol concentration in the scaled spectra, confirming the mixed cluster origin of the matched OH signals. Together with the evidence from Fig. S15, it is clear that there is only one dominant conformation of the 1:1 complex of EEK with methanol present in the expansion.

3 Comparison Experiment vs. Theory

Tab. S9: Using computed absorption cross-sections and the experimental integration ratios $\frac{I_1}{I_2}$ for complexes of methyl-ethyl-ketone (MEK) with MeOH, the docking ratios $\frac{c_1}{c_2}$ and resulting experimental docking fractions x_2 are derived. Entries with a * denote results based on the evaluation of difference spectra, to remove a minor methanol dimer contribution underneath sE. $\frac{I_1}{I_2}$ is obtained using an automated statistical evaluation.^{S8} Bounds for I_1/I_2 in MEK spectra are obtained from single bands and from the spectral noise hiding a hypothetical second band, using a quantile difference $q_{97.5} - q_{5.0}$ of the obtained distribution^{S9} (for more details on the evaluated spectra, see Fig. S17). Conformational freezing temperatures T_c are given, calculated with the ZPVE corrected DFT energy difference and $\frac{I_1}{I_2}$ from experiment, assuming unbiased theoretical absorption cross-sections. Error bars were obtained from upper and lower band integral ratio bounds and chosen symmetrically. For $\frac{I_1}{I_2}$ bounds based on single experimental signals, an upper value for T_c is derived. For the barriers expected in these systems, plausible T_c values are ≤ 150 K^{S10} and positive, but significantly higher than the rotational temperature of about 10 K. A higher T_c indicates an overestimated energy gap (or an unexpectedly high barrier) and a very low T_c indicates an underestimated energy gap.

Ketone	Method	E	$\frac{I_M}{I_E}$	$\frac{c_M}{c_E}$	x_E	$T_c^{\text{DFT}}/\text{K}$	T_c^{CC}/K		
MEK	B3LYP-D3	syn-E	3.8-4.6	3.4-4.2	0.19-0.23	207±15	92±7		
	B3LYP-D3	clinal-E	> 17.2	> 17.6	< 0.05	< 149	< 124		
	X3LYP-D3	syn-E	3.8-4.6	3.4-4.2	0.19-0.23	225±16	101±7		
	X3LYP-D3	clinal-E	> 17.2	> 17.3	< 0.05	< 134	< 125		
	X3LYP	syn-E	3.8-4.6	3.3-4.0	0.20-0.23	227±17	110±8		
	X3LYP	clinal-E	> 17.2	> 17.1	< 0.06	< 217	< 137		
	BP86-D3	syn-E	3.8-4.6	3.1-3.7	0.21-0.25	341±27	158±13		
	BP86-D3	clinal-E	> 17.2	> 17.7	< 0.05	< 173	< 104		
MEK*	B3LYP-D3	syn-E	5.1-6.6	4.6-5.9	0.15-0.18	166±12	74±5		
	B3LYP-D3	clinal-E	> 17.6	> 18.0	< 0.05	< 148	< 123		
	X3LYP-D3	syn-E	5.1-6.6	4.7-5.9	0.14-0.18	181±13	81±6		
	X3LYP-D3	clinal-E	> 17.6	> 17.8	< 0.05	< 133	< 124		
	X3LYP	syn-E	5.1-6.6	4.5-5.7	0.15-0.18	182±14	88±7		
	X3LYP	clinal-E	> 17.6	> 17.5	< 0.05	< 215	< 135		
	BP86-D3	syn-E	5.1-6.6	4.2-5.3	0.16-0.19	269±21	125±10		
	BP86-D3	clinal-E	> 17.6	> 18.1	< 0.05	< 172	< 103		
MEK	B3LYP-D3		$\frac{I_{sE}}{I_{cE}}$	$\frac{c_{sE}}{c_{cE}}$	x_{cE}				
			> 6.5	> 7.4	< 0.12	< 77	< 116		
			X3LYP-D3	> 6.5	> 7.3	< 0.12	< 43	< 112	
			X3LYP	> 6.5	> 7.4	< 0.12	< 161	< 123	
	BP86-D3	> 6.5	> 8.3	< 0.11	< 39	< 50			
	MEK*	B3LYP-D3		> 5.2	> 5.9	< 0.14	< 87	< 131	
				X3LYP-D3	> 5.2	> 5.8	< 0.15	< 48	< 126
				X3LYP	> 5.2	> 6.0	< 0.14	< 181	< 138
				BP86-D3	> 5.2	> 6.6	< 0.13	< 44	< 56

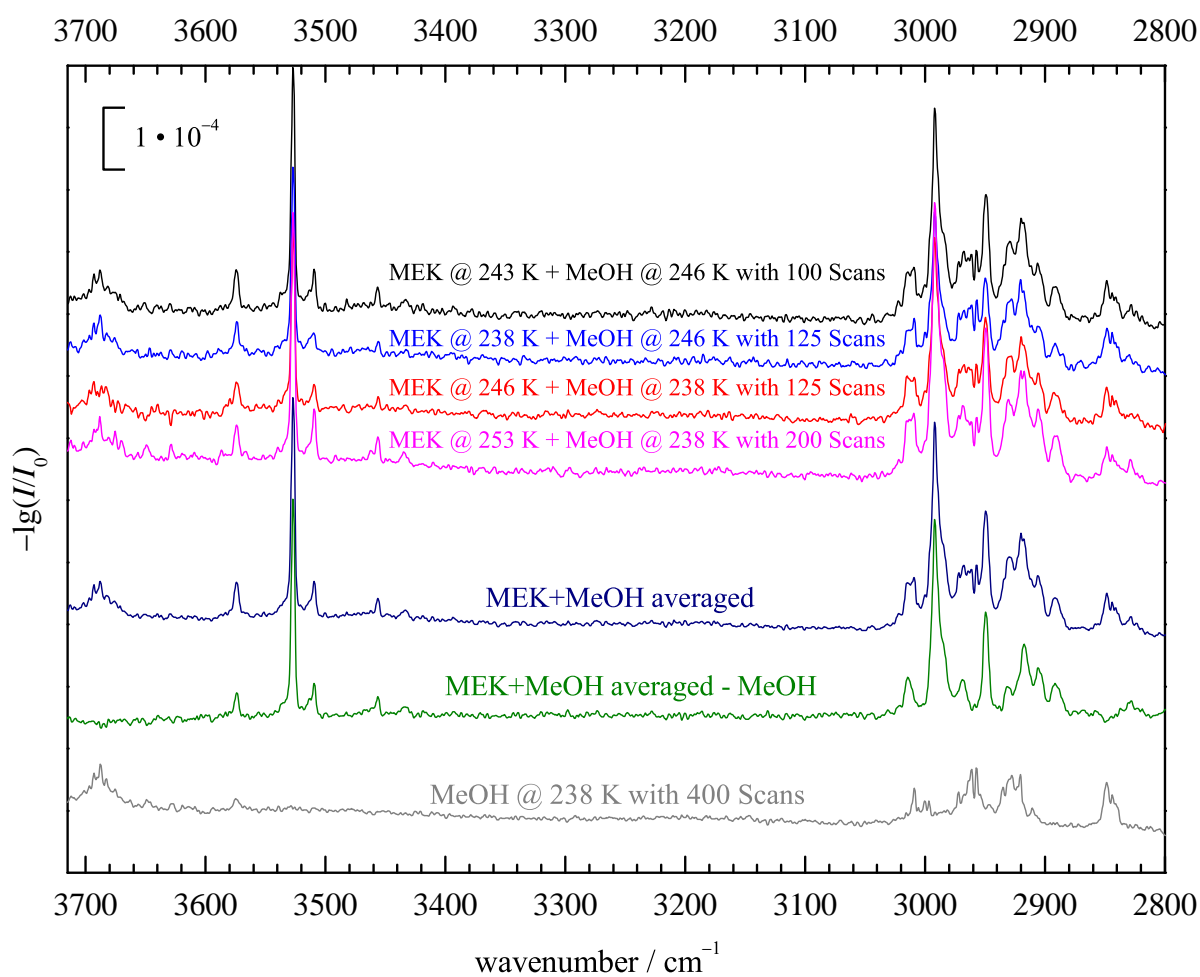


Fig. S17: FTIR jet OH stretching spectra of MEK in the presence of MeOH (black, blue, red, pink) at similar complex concentrations were averaged to obtain the dark blue spectrum (weighted average, MEK+MeOH averaged). Additionally provided is a pure MeOH spectrum with similar alcohol concentrations (gray) and the difference spectrum (green) used to obtain the experimental integration ratios in S9.

Tab. S10: Using computed absorption cross-sections and the experimental integration ratios $\frac{I_{sE}}{I_{cE}}$ for complexes of ethyl-ethyl-ketone (EEK) with MeOH, the docking ratios $\frac{c_{sE}}{c_{cE}}$ and resulting experimental docking fractions x_{cE} are derived. Entries with a * denote results based on the evaluation of difference spectra, to remove a minor methanol dimer contribution underneath sE. $\frac{I_{sE}}{I_{cE}}$ is obtained using an automated statistical evaluation,^{S8} while the bounds for $\frac{I_{sE}}{I_{cE}}$ in EEK spectra are obtained from single bands and from the spectral noise hiding a hypothetical second band, using a quantile difference $q_{97.5} - q_{5.0}$ of the obtained distribution^{S9} (for more details on the evaluated spectra, see Fig. S18). Conformational freezing temperatures T_c are given, calculated with the ZPVE corrected DFT energy difference and $\frac{I_{sE}}{I_{cE}}$ from experiment, assuming unbiased theoretical absorption cross-sections. For $\frac{I_{sE}}{I_{cE}}$ bounds based on single experimental signals, an upper value for T_c is derived. For the barriers expected in these systems, plausible T_c values are ≤ 150 K^{S10} and positive, but significantly higher than the rotational temperature of about 10 K. A higher T_c indicates an overestimated energy gap (or an unexpectedly high barrier) and a very low T_c indicates an underestimated energy gap (or a very low barrier). Indeed, comparison of Figs. S5 and S6 indicates a lower barrier for EEK. However, a cE signal hidden underneath the larger cluster bands should not be ruled out completely and would raise T_c .

Ketone	Method	E	$\frac{I_{sE}}{I_{cE}}$	$\frac{c_{sE}}{c_{cE}}$	x_{cE}	$T_c^{\text{DFT}}/\text{K}$	T_c^{CC}/K
EEK	B3LYP-D3	> 8.1	> 10.0	< 0.09	< 25	< 13	
	X3LYP-D3	> 8.1	> 9.9	< 0.09	< 3	< 1	
	X3LYP	> 8.1	> 9.6	< 0.09	< 74	< 11	
	BP86-D3	> 8.1	> 9.9	< 0.09	< 12	< 12	
EEK*	B3LYP-D3	> 7.6	> 9.3	< 0.10	< 26	< 14	
	X3LYP-D3	> 7.6	> 9.2	< 0.10	< 4	< 1	
	X3LYP	> 7.6	> 9.0	< 0.10	< 76	< 11	
	BP86-D3	> 7.6	> 9.2	< 0.10	< 12	< 12	

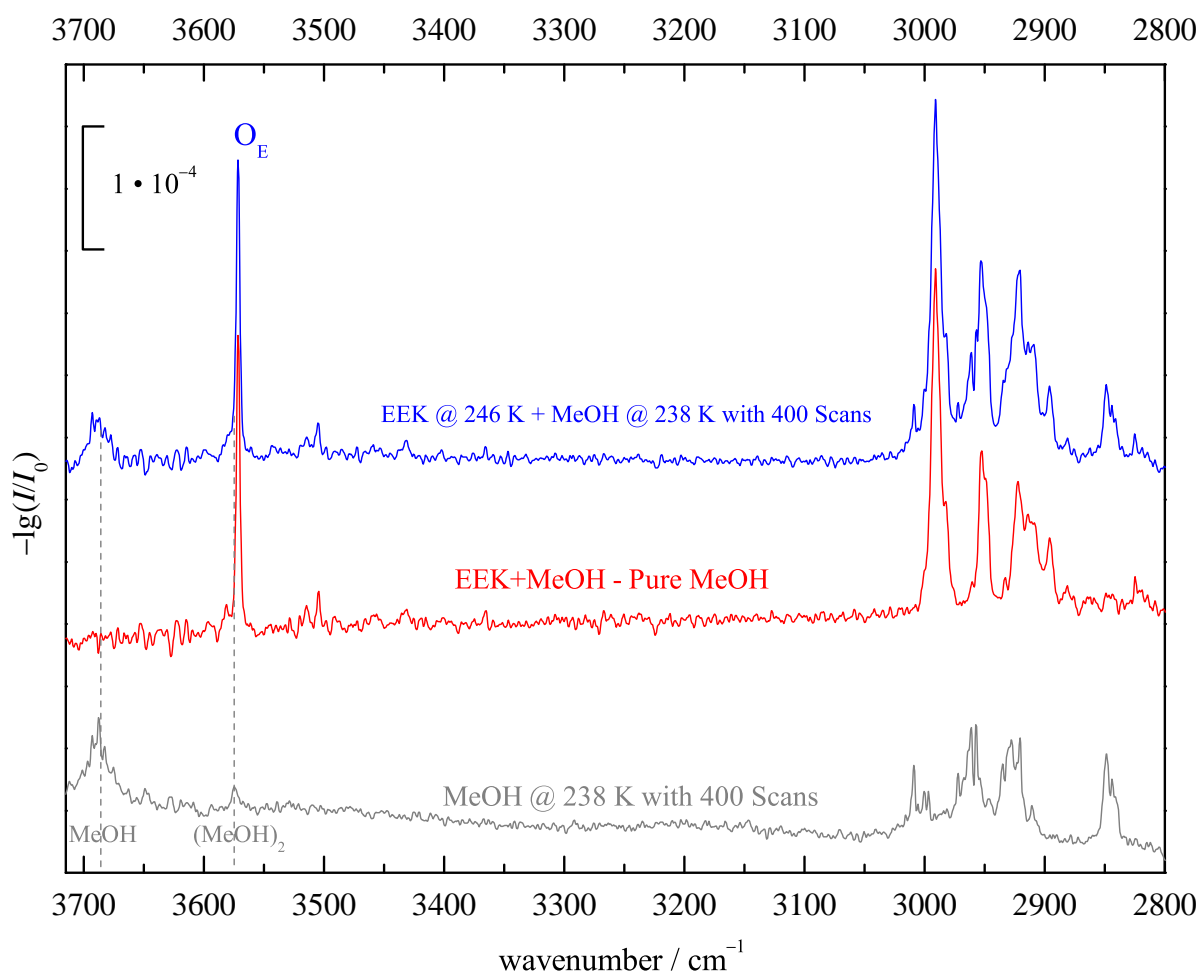


Fig. S18: FTIR jet OH stretching spectra of EEK in the presence of MeOH (blue) and a pure MeOH at similar alcohol concentrations (gray) are shown. Additionally, the difference spectrum for which the upper bounds for the experimental integration ratios in S10 are determined, is provided in red.

References

- (S1) Neese, F. Software update: the ORCA program system, version 4.0. *WIREs Comput. Mol. Sci.* **2018**, *8*, e1327.
- (S2) TURBOMOLE V7.3 2018, a development of University of Karlsruhe and Forschungszentrum Karlsruhe GmbH, 1989-2007, TURBOMOLE GmbH, since 2007; available from <http://www.turbomole.com>.
- (S3) Furche, F.; Ahlrichs, R.; Hättig, C.; Klopper, W.; Sierka, M.; Weigend, F. Turbomole. *WIREs Comput. Mol. Sci.* **2014**, *4*, 91–100.
- (S4) Goerigk, L.; Hansen, A.; Bauer, C.; Ehrlich, S.; Najibi, A.; Grimme, S. A look at the density functional theory zoo with the advanced GMTKN55 database for general main group thermochemistry, kinetics and noncovalent interactions. *Phys. Chem. Chem. Phys.* **2017**, *19*, 32184–32215.
- (S5) Moss, G. P. Basic terminology of stereochemistry (IUPAC Recommendations 1996):. *Pure Appl. Chem.* **1996**, *68*, 2193–2222.
- (S6) Kollipost, F.; Domanskaya, A. V.; Suhm, M. A. Microscopic Roots of Alcohol–Ketone Demixing: Infrared Spectroscopy of Methanol–Acetone Clusters. *The Journal of Physical Chemistry A* **2015**, *119*, 2225–2232, PMID: 24959926.
- (S7) Larsen, R. W.; Zielke, P.; Suhm, M. A. Hydrogen-bonded OH stretching modes of methanol clusters: A combined IR and Raman isotopomer study. *The Journal of Chemical Physics* **2007**, *126*, 194307.
- (S8) Karir, G.; Lüttschwager, N. O. B.; Suhm, M. A. Phenylacetylene as a gas phase sliding balance for solvating alcohols. *Phys. Chem. Chem. Phys.* **2019**, *21*, 7831–7840.
- (S9) Lüttschwager, N. O. B. NoisySignalIntegration.jl: A Julia package to determine uncertainty in numeric integrals of noisy x-y data. Available from GitHub.com: <https://github.com/nluetts/NoisySignalIntegration.jl>.

(S10) Poblitzki, A.; Gottschalk, H. C.; Suhm, M. A. Tipping the Scales: Spectroscopic Tools for Intermolecular Energy Balances. *J. Phys. Chem. Lett.* **2017**, *8*, 5656–5665.